



GLOBAL JOURNAL OF SCIENCE FRONTIER RESEARCH: A
PHYSICS AND SPACE SCIENCE
Volume 22 Issue 6 Version 1.0 Year 2022
Type: Double Blind Peer Reviewed International Research Journal
Publisher: Global Journals
Online ISSN: 2249-4626 & Print ISSN: 0975-5896

Gauge-Theoretic Study of Kundt Tube Experiment and Spontaneous Symmetry Transitions

By Tsutomu Kambe

University of Tokyo

Abstract- In the Kundt's experiment of acoustic resonance in closed tubes, two characteristic lengths were observed: one is the wave-length of the sound waves in resonance and the other the scale of dust striation. The latter has remained unresolved for its formation mechanism. Based on the Fluid Gauge Theory proposed recently by the author, formation mechanism of the dust striation is studied. When the sound is weak enough, the striation is unobserved. Once the wave intensity exceeds a threshold value, dust striations are formed. Formation of the dust striation is understood as a spontaneous transition of symmetry in the acoustics. According to the Theory, there is a transition of stress field within the fluid flow. Whereas the stress field is isotropic before transition, it becomes anisotropic after the transition. This is analogous to the spontaneous symmetry breaking known in the field theory. Lagrangian structures of both systems are verified to be analogous either.

GJSFR-A Classification: DDC Code: 813.54 LCC Code: PS3564.I362



Strictly as per the compliance and regulations of:



© 2022. Tsutomu Kambe. This research/review article is distributed under the terms of the Attribution-NonCommercial-NoDerivatives 4.0 International (CC BY-NC-ND 4.0). You must give appropriate credit to authors and reference this article if parts of the article are reproduced in any manner. Applicable licensing terms are at <https://creativecommons.org/licenses/by-nc-nd/4.0/>.

Gauge-Theoretic Study of Kundt Tube Experiment and Spontaneous Symmetry Transitions

Tsutomu Kambe

Abstract- In the Kundt's experiment of acoustic resonance in closed tubes, two characteristic lengths were observed: one is the wave-length of the sound waves in resonance and the other the scale of dust striation. The latter has remained unresolved for its formation mechanism. Based on the Fluid Gauge Theory proposed recently by the author, formation mechanism of the dust striation is studied. When the sound is weak enough, the striation is unobserved. Once the wave intensity exceeds a threshold value, dust striations are formed. Formation of the dust striation is understood as a spontaneous transition of symmetry in the acoustics. According to the Theory, there is a transition of stress field within the fluid flow. Whereas the stress field is isotropic before transition, it becomes anisotropic after the transition. This is analogous to the spontaneous symmetry breaking known in the field theory. Lagrangian structures of both systems are verified to be analogous either.

I. INTRODUCTION

In the middle of the 19th century, August Kundt carried out acoustic experiments to estimate sound speeds in various gases and materials, in laboratories very innovatively, from wave phenomena of sound resonance excited in closed tubes and published those observations in 1866 [1]. In this paper he reported an anomaly which has remained unresolved for a long time. The issue was as follows: there existed two characteristic scales, observed in his experiment. One is the wave-length of the sound wave in resonance within the tube, which was just the one being sought in his experiment. However embarrassingly to him, another characteristic scales were observed in his experiment, *i.e.* the dust striations formed in the resonant standing waves which were characterized with much shorter scales. Formation mechanism of the second dust striation has remained unresolved, *i.e.* without being given an appropriate interpretation on its physical mechanism.

After more than eighty years since then, in 1955 Robert Carman wrote a very informative review [8] for teachers of physics and explained compactly the *Kundt Tube Dust Striations*. Showing a beautiful sketch of striations, he noted that very few know what to say when a student asks why the dust figures in the tube are striated.

Most frequently offered explanations were that those were caused by higher harmonics of the resonant mode. But this was refuted by Dvorak [2] already in 1874. He argued that a very high overtone would be necessary to explain the observed wavelength of about 0.8cm for a typical resonant wavelength of about 11cm of Kundt's experiment. It is unconceivable in mechanics to assume that only one overtone is sufficiently stronger than any others to produce such distinct ripples.

Author: Former Professor, University of Tokyo, Hongo, Bunkyo, Tokyo, Japan. e-mail: kambe@ruby.dti.ne.jp
The main part of present study was presented orally at the Physics-2022 held at San Francisco, USA, on 18 - 21 July 2022.

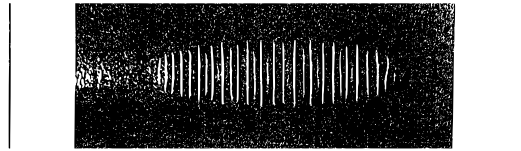


Fig. 1: Experimental picture of dust striation from Fig.7 of [7]. The two vertical bars on both sides are the part of Fig.7, signifying the length between them corresponds to $\frac{1}{2} \lambda_r$.

In this regard, the experimental studies of Andrade ([5]~[7]) are particularly noteworthy. Those were carried out prior to Carman's review (1955). In 1931, since it had passed already 65 years from the Kundt's work [1], the experimental devices of Andrade were renewed significantly with using electric oscillators and vibrating diaphragms, enabling steady-state conditions maintained during the observation of Andrade. Thus he was able to lower the resonance frequencies to 100 to 2300 cps (compared with previous values, 2500 ~ 4000). As viewed from the present time, his key findings were two:

- (i) A certain minimum velocity of the air particles is required for the ripple formation;
- (ii) The inception of ripple formation corresponds to a spontaneous breakdown of the physical state of vortex-free flow in the tube.

The first signifies that there is a critical intensity of sound for the formation and the second implies that the ripple formation resulted from a spontaneous symmetry breaking. These findings are reviewed in the present study from the fluid-dynamic point of view on the basis of the Fluid Gauge Theory [13]. This is one of the main issues.

Kundt's experiment attracted interest of Rayleigh [4], who proposed that, within a sinusoidal standing wave excited powerfully in a pipe, steady streaming is generated in addition to the periodic oscillation by the action of the nonlinear mean Reynolds stress in collaboration with the dissipative dragging action of viscosity. Andrade [6] presented experimental photographs showing this steady streaming (Fig. 5(a)). In these backgrounds, Lighthill showed a diagram of the steady streaming ([11], Fig. 85) consisting of four cells of closed streamlines within a wavelength λ_r , noting that this explains why dust particles tend to accumulate at the nodes and there are two nodes within λ_r .

However, it is noted by Andrade [7] that the steady streaming is observed only under prolonged intensive sound waves. Lowering the intensity, but still above a critical intensity, he observed ripple-like striation with using minute cork particles. FIG.1 is its photo from [7], showing a number of ripple waves within a half wavelength $\frac{1}{2} \lambda_r$. Kundt himself [1] used a number of minute Lycopodium dried spores as the dust particles, and described the structure of lateral striation as *ribs*, which were caused by the air in motion, not by other causes. Since then, very little is known about its formation mechanism.

The Kundt-tube experiments show us various interesting acoustic phenomena. Therefore, the present approach investigates the Kundt-tube experiments from diverse aspects: (a) *fluid-mechanically*, concerning stress fields, transition from a stress field to another, oscillatory boundary layers over the tube walls, or steady streaming as a nonlinear effect; (b) *gauge-theoretically*, concerning Lagrangians, gauge fields, or spontaneous symmetry transition.

First in the sections II and III, various phenomena observed in the experiments are presented compactly and then reviewed from a gauge-theoretic point of view, emphasizing that a transitional change of acoustic phenomena may be interpreted as spontaneous symmetry

transition. Then in § IV, the *fluid gauge theory* is presented for its theoretical interpretation. Computer simulations are also presented to visualize non-trivial acoustic phenomena occurring within the flow fields in § III and IV, helped by the experimental picture (FIG.2) of the rotational eddy field visualized by Andrade [7].

In the flow fields studied here, there are three types of stress fields (§ IV-C) which are playing important roles in the acoustic phenomena: (A) *isotropic* stress field $\sigma_1^{jk}(x^\nu)$ (non-dissipative), (B) *anisotropic* stress $\sigma_A^{jk}(x^\nu)$ (non-dissipative), and (C) *viscous* stress $\sigma_{vis}^{jk}(x^k)$ (anisotropic and dissipative). Traditional Eulerian fluid system is governed by the isotropic pressure stress σ_1^{jk} . Depending on whether the stress field is isotropic σ_1^{jk} or anisotropic σ_A^{jk} , the fluid current field $j^\mu(x^\mu)$ changes its character drastically. In fact, this is one of the main themes of the present study. The third viscous stress σ_{vis}^{jk} plays an important role in the Navier-Stokes system.

The viscous stress tensor has anisotropic components as well. The anisotropic components of viscous stress play essential roles in the study of fluid mechanics. Turbulence theory learns those and takes advantage of the anisotropic property of viscous stress. However, there exists an essential difference between the two fields of the viscous stress σ_{vis}^{jk} and the FGT anisotropic stress $\sigma_A^{\nu k}$. The former is dissipative (shown in § IV (3)), while the latter is conservative because the mechanical systems derived from the action principle in terms of Lagrangians (§ IV, A and B) have Hamiltonian system of equations of motion which conserve the total mechanical energy (*cf.* [19] § 2.3; [20] § 2.3). Hence the present study emphasizes the importance of the conservative stress field $\sigma_A^{\nu k}$. This is another theme of the present.

Section V reviews the theory of steady streaming generated by oscillatory boundary layers in the acoustic system, which is also observed in the Kundt's system [7].

Section VI investigates a similarity of spontaneous symmetry transitions occurring in two quite-different physical systems: (a) Kundt's acoustic system and (b) Higgs' mechanism ([21], [22]). It is quite unexpected finding that an analogy exists between the Lagrangian structures of both systems. Each system is described by a triplet of Lagrangians, each of which has similarity respectively. Most obvious similarity is seen in the forms of the Lagrangian describing interactions (see § VI).

II. BRIEF DESCRIPTION OF KUNDT'S EXPERIMENT BY FLUID GAUGE THEORY

The *present* study takes new fluid-mechanical view-points in order to describe the Kundt's experiment with physical terms. In particular, to explain the two experimental observations (i) and (ii) given in the Introduction, the *Fluid Gauge Theory* [13] is applied to those observations. The application has been found very successful. The outcomes obtained by the application have disclosed two innovative aspects of the Kundt's acoustic system. Such new findings are presented compactly in this section but detailed analyses are postponed to the following sections. The two innovative findings are as follow.

(I) Firstly, it is understood that the formation of dust striation in the Kundt's experiment tells a deep message. Namely, according to the theory [13], the *dust striation* shows an experimental evidence of existence of a background gauge field in the acoustics, characterized with much shorter scales of the striation. The theory predicts that trace of the background gauge field had been visualized with the dust striations.

(II) Secondly, by detailed examinations of the experiment and the theoretical structures, the Fluid Gauge Theory implies an unexpected finding that the formation mechanism of

Kundt's dust striation is analogous to the spontaneous symmetry breaking, known in the Higgs mechanism. This is found by comparing the Lagrangian structure of the Fluid Gauge Theory with that of Higgs mechanism (see the section VI). Formation of Kundt's dust striation is in fact an acoustic analogue of *Spontaneous Symmetry Breaking* (Nambu [23]).

August Kundt [1] noted a remarkable statement in 1866 as follows: *As far as the origin of these transverse ribs is concerned, I refrain from any statement at this point. I would therefore prefer not to attempt its explanation at all, nor give an explanation, which I am forced to withdraw later.* Concerning the experimental evidence, this implies that he knew clearly the whole of phenomena, but realized that he was unable to find any appropriate theory to explain it.

As a possible theory, the Fluid Gauge Theory [13] is presented to explain the formation mechanism. The theory is formulated on the bases of two sets of 4-vector fields: (i) *Fluid current 4-vector* $j^\mu(x^\nu)$ and (ii) *Background gauge-field 4-covector* $a_\mu(x^\nu)$ ($\mu, \nu = 0, 1, 2, 3$). Regarding the gauge field $a_\mu(x^\nu)$, a preliminary comment is given below in this section with detailed definitions postponed to later sections.

The Fluid Gauge Theory (FGT in short) is formulated in terms of relativistic Lagrangians, and hence the current 4-vector $j^\mu(x^\nu)$ is defined relativistically as follows:

$$j^\nu = \rho(c, \mathbf{v}) = c\bar{\rho}u^\nu, \quad u^\nu \equiv dx^\nu/d\tau, \quad \bar{\rho} = \rho\sqrt{1-\beta^2}, \quad (1)$$

with c the light velocity, ρ the fluid mass density, \mathbf{v} the fluid velocity in 3-space and $\beta \equiv |\mathbf{v}|/c$.¹ Concerning the Fluid-Mechanics, the *following* observation is instructive. Namely *there exist glimpses of linked structure of 4d-space-time*, represented by 4d inner products:

$$\partial_\nu j^\nu = \partial_t \rho + \nabla \cdot (\rho \mathbf{v}); \quad j^\nu \partial_\nu = \rho(\partial_t + \mathbf{v} \cdot \nabla) \equiv \rho D_t, \quad (2)$$

where $\partial_\nu = (c^{-1}\partial_t, \nabla)$, and $D_t = \partial_t + \mathbf{v} \cdot \nabla$. The first is nothing but the expression leading to the *continuity equation* ($\partial_\nu j^\nu = 0$), and the second $D_t \equiv \partial_t + \mathbf{v} \cdot \nabla$ the *material derivative*.

The reason why the gauge field $a_\mu(x^\nu)$ is introduced in the FGT theory is to ensure the continuity equation $\partial_\nu j^\nu = 0$ which should be deduced from the action principle of invariant variation, instead of writing it *a priori*. Namely, the continuity equation is not given *a priori*, but is ensured owing to the existence of the gauge field $a_\mu(x^\nu)$.

Initially when the sound wave was weak, the system is governed by the traditional Eulerian system, but accompanying a *transparent* (invisible) gauge field a_ν (see below). As the wave intensity increases, the gauge field shows spontaneously its appearance at a transition when the field is colored with a rotational field superimposed on the transparent field. In fact, the traditional Eulerian system works only under such transparent gauge fields.

The present *Fluid Gauge Theory* [13] has been formulated according to the *gauge principle* of general gauge theory ([15], [16]), and the present theory extends the *isotropic* pressure stress fields σ_τ of the traditional Eulerian fluid system to *anisotropic* stress fields σ_λ at a transition caused by a certain physical mechanism (which will be considered in the section III, helped with computer simulations).

¹ $\mu, \nu = 0, 1, 2, 3$. The *overlined* value $\bar{\rho}$ denotes the *proper* value (*i.e.* the density ρ in the *rest frame* where the fluid is at rest). For the proper time τ , $d\tau \equiv \sqrt{1-\beta^2} dx^0$ where $x^\nu = (ct, \mathbf{x})$ with $x^0 = ct$, t the time. and $\mathbf{x} = (x^1, x^2, x^3)$ a 3-vector notation. Following notations are used: $d^3x \equiv dx^1 dx^2 dx^3$, and $\nabla = (\partial_k)$ where $\partial_k = \partial/\partial x^k$, $k = 1, 2, 3$. The metric tensor is $\eta_{\mu\nu} = \eta^{\mu\nu} = \text{diag}(-1, 1, 1, 1)$.

III. TRANSITION OF STATES

Let us consider *fluid-dynamic* aspects of the Kundt's experiment by examining the stress fields. Suppose that the air in a closed tube is excited with resonant sound waves. During the initial period when the sound intensity is weak, main part of the air motion executes longitudinal oscillation, which is vortex-free and irrotational. This is described very nicely by the Euler's system of an ideal fluid without viscosity. However, as the sound intensity increases, presence of minute dust particles scattered over the lower tube-wall acts as source of eddy, providing rotational component to the main part. This plays a certain role of trigger that prompts the state transition.

a) *Transition is prompted by fluid-mechanical processes*

As the sound intensity increases in the tube, the *rms* velocity $\bar{u} = \langle |\mathbf{u}_m|^2 \rangle^{1/2}$ of the air motion increases where $|\mathbf{u}_m|$ is a representative magnitude of velocity of air-gas molecules. Presence of dust particles within intense acoustic field favors transition of the stress field within the oscillating air to another stress field of different characteristics. Suppose that there exist small external objects acting as roughness on the wall. When the air is flowing fast over the roughness surface, its boundary layer separates from the solid roughness surface if an effective Reynolds number of the fluid motion is sufficiently high to enable the flow separation, as verified experimentally in [6]. Then, shearing rotational flows are supplied within the fluid, inducing eddying fluid motion within a broader space region. This was studied experimentally by Andrade ([5] ~ [7]).

In 1930s, Andrade carried out detailed studies on the Kundt's experiment with updated devices at his times. From his earlier studies, he concluded on the basis of the Reynolds numbers observed experimentally that the periodic air motion about an obstacle produced eddying motion. This rotational motion was mixed and combined with the surrounding irrotational oscillating motion in the pipe. Concerning all the previous experiments carried out not only by himself but also by other previous workers, he commented that the air motion previously had been assumed tacitly to be irrotational, but actually the motion had been rotational.

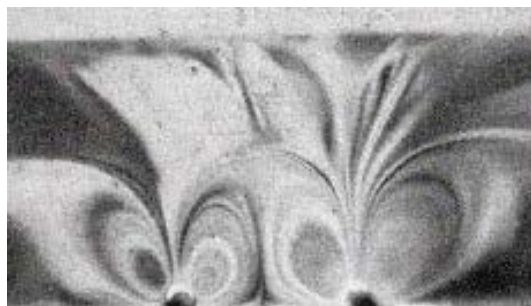


Fig. 2: Photo of eddies visualized with smoke ([7], Fig.27). On the lower wall two thin cylinders (seen dark) were placed and the upper wall seen as white belt.

Figure 2 shows one of the many photos in the paper [7], visualizing eddy pattern (with using tobacco smoke) generated by a pair of thin cylinders placed at the bottom transversally (perpendicular to the sheet) within the resonant longitudinal (*left-right*) air motion. Andrade gave a plenty of experimental evidences in [7] of existence of eddying motions generated by obstacles in the field or roughness elements on the lower wall. In the absence of roughness

or obstacles, the air oscillation should be longitudinal and mainly irrotational external to thin boundary layers (caused by the non-slip condition of viscosity effect).

Hinted by the experimental evidences of Andrade, we can make a following observation on the acoustic field of Kundt's experiment. Those experimental evidences imply that there must have been a *transition* in the acoustic field when the sound intensity was made increased.

b) Prediction of the FGT theory

In the traditional Fluid Mechanics, the fluid is said to be *ideal* if its mechanical energy is conserved during its motion, and said *dissipative* if its kinetic energy is lost into heat energy by the action of viscosity. The equation of motion of the air (assumed to be an ideal non-dissipative fluid as an idealization) is given by the form:

$$\rho D_t v^k = -\partial_k p, \quad k = 1, 2, 3, \quad (3)$$

where p is the pressure, v^k is the k -th component of the fluid velocity, and the operator $D_t \equiv \partial_t + \mathbf{v} \cdot \nabla$ is the material derivative defined by (2).

In the present problem of the state transition, we are interested in the stress field $\sigma^{jk}(\mathbf{x})$ within the space of acoustic resonance, By using it, the above equation of motion can be rewritten as

$$\rho D_t v^k = \partial_j \sigma_1^{jk}, \quad \sigma_1^{jk} = -p \delta^{jk}, \quad (j, k = 1, 2, 3), \quad (4)$$

where σ_1^{jk} is the stress tensor representing the *Isotropic* pressure stress.² The equation (4), or equivalently (3), is nothing but the Euler's equation of motion.

The Fluid Gauge Theory (briefly described in §II) predicts transition of the stress field in the fluid in motion. This implies that the form of σ_1^{jk} given in (4) may take another form at a certain transition. There are three types of stress fields (to be considered below in the current issue): (A) *isotropic* stress field $\sigma_1^{jk}(x^\nu)$ (non-dissipative), (B) *anisotropic* stress $\sigma_A^{jk}(x^\nu)$ (non-dissipative), and (C) *viscous* stress $\sigma_{\text{vis}}^{jk}(x^k)$ (anisotropic and dissipative). As mentioned briefly in the section II, the traditional Eulerian fluid system, governed by the isotropic pressure stress σ_1^{jk} , works under transparent gauge fields.

When sound intensity is weak, Euler's equation of motion (4) is valid, with the stress field represented by the isotropic stress σ_1^{jk} . Interestingly, the same Eulerian Fluid system is valid in the Fluid Gauge Theory when the gauge field a_ν is transparent, *i.e.* when a_ν is expressed as $\partial_\nu \Psi(x^\mu)$. This finding gives a hint to develop a new theory.

In the Kundt's experiment of acoustic resonance, when the sound intensity was increased, minute dust-like particles of random dispersion showed unexpected behaviors under the acoustic field. The cluster of dust particles arranged themselves spontaneously and formed transversal rib-like structure having much smaller scale than the wavelength λ_r of resonant waves. This is understood as *spontaneous symmetry transition*.

² A tensor of the form $p \delta^{jk}$ is said an isotropic tensor, since the metric tensor in the $3d$ cartesian space is given by the isotropic tensors: $\delta^{jk} = \delta_{jk} = \text{diag}(1, 1, 1)$. Then, raising the lower index of ∂_k is simply done by $\partial^k = \delta^{kl} \partial_l$. Then the equation (3) can be rewritten as $\rho D_t v^k = -\partial^k p$.

An extension from the transparent gauge field $a_\nu^{(0)} = \partial_\nu \Psi$ to general gauge field a_ν , *i.e.* general 4-vector field $a_\nu(x^\mu)$, is enabled by the *principle of local gauge invariance* according to the General Gauge Theory ([13], [15], [16]). This is described in the section IV. In fact, the new general gauge field a_ν enforces transition of the stress field from the *isotropic* σ_1^{jk} to *anisotropic* stress field σ_A^{jk} of the system, given by (21) \sim (23). This is called the *Fluid Gauge Theory* (in short, *FGT*). The former stress field σ_1^{jk} has affinity with *irrotational* velocity field under the transparent field $a_\nu^{(0)}$, while the latter stress field σ_A^{jk} is receptive with *rotational* (eddy) velocity field in combination with the colored field $a_\nu(x^\mu)$. This is consistent with what is explained in the above paragraph for the experimental visualization of the rib-like structure of dust particles existing in the acoustic field, called the *spontaneous symmetry transition*.

c) Comparison of Flow Fields before and after the Transition

In order to see the difference of the flow fields before and after the transition of stress field, let us carry out simple model analyses in this section. Consider a fluid in $2d$ (x, y) -channel with the channel axis taken to the x -direction and its width H to the normal y -direction.

Before the transition, the motion is governed by the equation (4) under the isotropic pressure stress σ_1^{jk} . In this analysis, no-slip condition is applied on both of the upper and lower walls, so that the viscous stress term σ_{vis}^{jk} is added³. The equation of motion takes the following form, *i.e.* the Navier-Stokes equation:

$$\rho D_t v^k = \partial_j \sigma_1^{jk} + \partial_j \sigma_{\text{vis}}^{jk}. \quad (5)$$

The fluid motion is assumed to be *unidirectional*: $\mathbf{v} = (u(t, y), 0, 0)$. Instead of sound oscillation in the channel, an analogous problem is chosen by taking special boundary conditions with the lower wall $y = 0$ being in motion under no-slip condition (moving in its own plane), while the upper wall $y = H$ is kept at rest. More precisely, the lower wall is given a time periodic motion of a period T and a space-periodic tangential motion of wavelength λ_g , and its x velocity is given by⁴

$$u = u_w \sin 2\pi(x/\lambda_g) \cos 2\pi(t/T).$$

To see the characteristic features of fluid motion before the transition, the equation (5) was solved under the stresses, $\sigma_1^{jk} + \sigma_{\text{vis}}^{jk}$, satisfying the boundary conditions mentioned above.

Next, after the transition, according to the last paragraph of section (b), the *anisotropic* stress field σ_A^{jk} is newly added and the total stress field takes the form $\sigma_1^{jk} + \sigma_A^{jk} + \sigma_{\text{vis}}^{jk}$, where the form of σ_A^{jk} is defined by (22) and (23) in the next section IV. Hence the equation of motion (4) is replaced by

$$\rho D_t v^k = \partial_\nu \sigma_1^{\nu k} + \partial_\nu \sigma_A^{\nu k} + \partial_j \sigma_{\text{vis}}^{jk}. \quad (6)$$

To see the fluid motion after the transition, the equation (6) was solved under the same driving condition at the lower wall $y = 0$ while taking passive condition at the upper wall, taking reflection-less boundary condition allowing slip.

³ $\sigma_{\text{vis}}^{jk} = 2\eta(e_{jk} - \frac{1}{3}\Delta\delta_{jk})$. where η is a viscosity coefficient, $e_{jk} = \frac{1}{2}(\partial_j u_k + \partial_k u_j)$ and $\Delta = e_{kk}$.

⁴ where $u_w/c_s = 1.5 \times 10^{-3}$ and $c_g/c_s = 0.031$ for c_s sound speed (344 m/s at 20° C) and c_g speed of gauge field.

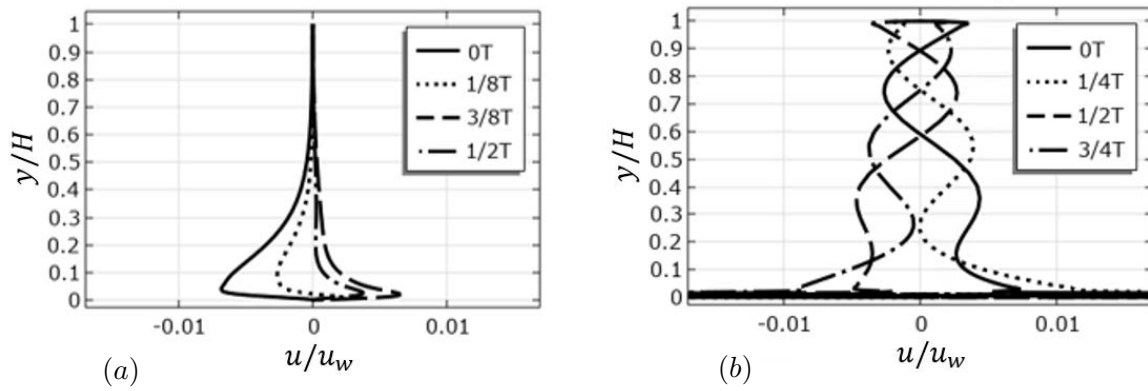


Fig. 3: Comparison of velocity fields generated by different stress fields at $x/\lambda_g = 0.45$: (a) before the transition and (b) after the transition. See Appendix B 4 for more details.

Figure 3 compares the flow developments before (left) and after (right) the transition in 2d (x, y) -channel within a period T of oscillation. The figure on the left is the Stokes-type oscillatory layer (Eulerian + viscosity: under transparent gauge field), while that on the right is the wavy layer in FGT system (FGT+viscosity under general colored gauge field).

Difference of the features of both fields is remarkable. This impressive difference has been caused by the transition of internal stress field from the isotropic σ_I^{jk} to the anisotropic σ_A^{jk} , which may be called as *Spontaneous Symmetry Transition*.

d) Effect of the anisotropic stress field $\sigma_{(ani)}^{jk}$

Under the influence of anisotropic stress field σ_A^{jk} , the acoustic field is modified spontaneously. In the Kundt's experiment, when the sound intensity was increased, the cluster of minute dust particles arranged themselves spontaneously forming rib-like structure of much smaller scale than the resonant wavelength λ_r .

On the basis of the FGT theory, computer simulation has been carried out. Figure 4 shows computed streamlines in the acoustic field averaged over a cycle of sound oscillation. Striking similarity is observed between the two of FIG.2 and FIG.4, concerning the envelope curves seen at the central lower part of the figures, both of which enclose a pair of eddies with their heights reaching half of the channel height. This is remarkable because the experimental photo of FIG.2 was taken in 1930s by Andrade ([5]~[7]) visualizing the flow pattern by tobacco smoke, while the computed envelope line of FIG.4 has been obtained in

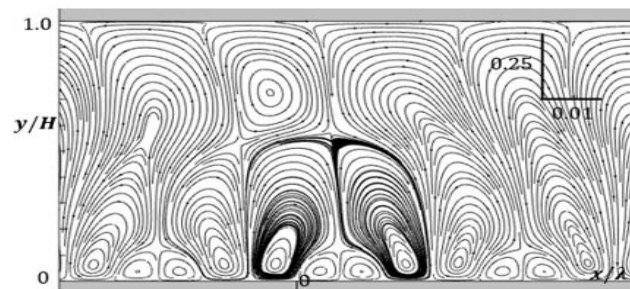


Fig. 4: Streamlines computed from the velocity field of FGT theory averaged over a cycle of acoustic oscillation .

this year by the FGT theory presented next in the section IV, or by the governing system of equations (21) ~ (23) of § IV C-2,⁵ under the time separation of ninety years.

Another point to be remarked is that this structure was sketched and shown as the figure 2 of [7], in order to illustrate formation of small intermediate ridges (libs) of dust which are seen in FIG.1 as shorter vertical lines between longer ones. In FIG.4, the shorter line corresponds to the innermost eddy-pair surrounded by outer larger pair of eddies. In FIG.2, there must be a separation bubble of eddies although it is hard to recognize.

Thus it is understood that longitudinal (*left-right*) sequential array of transversal eddies of FIG.4 are responsible for formation of the Kundt's dust striation.

IV. FLUID GAUGE THEORY (FGT)

The *Fluid Gauge Theory* [13] has been proposed to improve representation of the stress fields within fluid flows including strong turbulence, by extending the isotropic pressure stress field $\sigma_1^{\nu k}$ to anisotropic stress field $\sigma_A^{\nu k}$. As explained in the previous sections II and III for the formation mechanism of Kundt's dust striations, it is remarkable that this new gauge theory is found to explain most appropriately the fluid mechanical aspects of what are happening in the resonance tube of Kundt's experiment. Therefore, its detailed theoretical structure is presented in this section.

a) *Lagrangians*

Total Lagrangian \mathcal{L}^{FGT} proposed by the FGT theory [13] for the fluid system consists of three parts, $\mathcal{L}^{\text{FGT}} = \mathcal{L}_{\text{fluid}} + \mathcal{L}_{\text{int}} + \mathcal{L}_a$:

$$\mathcal{L}_{\text{fluid}} = -c^{-1}(c^2 + \bar{\epsilon}(\bar{\rho}))\bar{\rho}, \quad (7)$$

$$\mathcal{L}_{\text{int}} = c^{-1}j^\nu a_\nu, \quad (8)$$

$$\mathcal{L}_a = -(4\mu c)^{-1}f^{\nu\lambda}f_{\nu\lambda}, \quad (9)$$

$$f_{\nu\lambda} \equiv \partial_\nu a_\lambda - \partial_\lambda a_\nu, \quad \bar{\rho} \equiv \rho\sqrt{1 - \beta^2}, \quad (10)$$

where $\beta \equiv |\mathbf{v}|/c$, and *overlined* values denote proper values. The action of the system S^{FGT} is defined by

$$S^{\text{FGT}} \equiv \int \mathcal{L}^{\text{FGT}} d\Omega = \int [\mathcal{L}_{\text{fluid}} + \mathcal{L}_{\text{int}} + \mathcal{L}_a] d\Omega, \quad (11)$$

where $d\Omega = c dt d^3x$. The first $\mathcal{L}_{\text{fluid}}$ is the Lagrangian of a perfect fluid (*i.e.* an ideal fluid). In fact, in non-relativistic limit as $\beta \rightarrow 0$, the expression of $\mathcal{L}_{\text{fluid}} c d^3x$ per unit mass ($m_1 \equiv \rho d^3x = 1$) reduces to the non-relativistic Lagrangian, $L_{nr} \equiv \frac{1}{2} m_1 v^2 - \epsilon$ (with ϵ the specific internal energy), neglecting the rest-mass energy $-m_1 c^2$. Hence it is seen that the Lagrangian $\mathcal{L}_{\text{fluid}}$ is a relativistic version extended from the classic non-relativistic form L_{nr} .

The third \mathcal{L}_a is the Lagrangian of the gauge field represented in a form satisfying local gauge invariance with respect to the gauge field a_ν as well as ensuring current conservation. The middle \mathcal{L}_{int} represents the interaction between the current j^ν and the gauge field a_ν .

⁵ This test simulation was done by $-\partial_t \mathbf{d} + \nabla \times \mathbf{h} = \rho \mathbf{v}$ (see (16)) for the gauge field a_ν and the equation of motion (6) with additional viscosity stress σ_{vis}^{jk} , under the approximation $|\rho'/\rho| \ll 1$ and $|\nabla \phi / \partial_t \mathbf{a}| \ll 1$.

Equations of motion are deduced from the action principle and the force field is represented in terms of the stress field σ .

b) *Governing equations*

To find the equations of motion, the action principle is applied to S^{FGT} , by assuming the gauge field a_ν given and vary only the position coordinate x_p^k of fluid particles moving with the velocity $v^k = D_t x_p^k$ along their trajectories ($k = 1, 2, 3$). In the non-relativistic limit as $\beta \rightarrow 0$, the equation of motion is deduced by the action principle as

$$\rho D_t v^k = -\partial^k p + \rho f^{k\nu} v_\nu, \quad (k = 1, 2, 3), \quad (12)$$

(cf. Eq.(2.30) of [13]) from the combination of two Lagrangians $\mathcal{L}_{\text{fluid}}$ and \mathcal{L}_{int} , since the third \mathcal{L}_a is invariant in this variation. By the (0, 3)-notation, we have $v_\nu = (-c, \mathbf{v})$ and $v^\nu = (c, \mathbf{v})$ with \mathbf{v} being a 3-vector, and $\nu = 0, 1, 2, 3$ must be taken in (12).

To find the equations governing the gauge field a_ν , we vary only the field a_ν with assuming the fluid motion $j^\nu = \rho v^\nu$ given. From the action principle, we obtain

$$\frac{\partial}{\partial x^\lambda} f^{\nu\lambda} = \mu j^\nu \quad (13)$$

(see Eq.(2.32) of [13]) with $j^\nu = (\rho c, \mathbf{j})$ and $\mathbf{j} = \rho \mathbf{v}$, where μ is a control parameter (introduced in (9)) to denote the degree of mutual interaction.

The equation of current conservation can be derived from this, which is directly connected with the gauge-invariant property of the Lagrangian \mathcal{L}_a (see [14], § II (a)). This is analogous to the electromagnetic fields. In fact, applying the divergence operator ∂_ν on the equation (13), one obtains $0 = \partial_\nu \partial_\lambda f^{\nu\lambda} = \mu \partial_\nu j^\nu$. The middle side of total summation with respect to ν and λ vanishes because of the anti-symmetry of $f^{\nu\lambda}$ and the symmetry of $\partial_\nu \partial_\lambda$ with respect to ν and λ . Hence, the current conservation equation is deduced:

$$\partial_\nu j^\nu = 0, \quad \Rightarrow \quad \partial_t \rho + \nabla \cdot (\rho \mathbf{v}) = 0, \quad (14)$$

(see (2)). The third Lagrangian \mathcal{L}_a ensures the *mass conservation*.

Introducing the (0, 3)-notation for a_ν too (like below (12)) by $a_\nu = (-\bar{\phi}, \mathbf{a})$ where $\bar{\phi} \equiv \phi/c$ for ϕ a scalar field, we define new two 3-vector fields \mathbf{e} and \mathbf{b} by

$$\mathbf{e} \equiv -\partial_t \mathbf{a} - \nabla \phi, \quad \mathbf{b} \equiv \nabla \times \mathbf{a}. \quad (15)$$

Then, these enable the equation (13) transformed into a pair of equations analogous to the Maxwell equations of *Electromagnetism*. In fact, with defining \mathbf{d} and \mathbf{h} by $\mathbf{d} = \epsilon \mathbf{e}$ and $\mathbf{h} = \mathbf{b}/\mu$ with using $\epsilon \equiv 1/(\mu c^2)$, the equation (13) gives a pair of Maxwell equations:

$$-\partial_t \mathbf{d} + \nabla \times \mathbf{h} = \mathbf{j}, \quad \nabla \cdot \mathbf{d} = \rho, \quad (16)$$

(Eq.(3.18) of [13]). Definition (15) gives another pair of Maxwell equations (Eq.(3.20) of [13]):

$$\partial_t \mathbf{b} + \nabla \times \mathbf{e} = 0, \quad \nabla \cdot \mathbf{b} = 0. \quad (17)$$

In summary, it is found that the fluid current field $j^\mu(x^\mu)$ changes its character drastically, depending on whether the gauge field a_ν is derived from a scalar potential $\Psi(x^\mu)$ (i.e. $a_\nu = \partial_\nu \Psi$) or takes an intrinsic 4-vector form $a_\nu(x^\mu)$ yielding non-vanishing $f_{\mu\nu} (= \partial_\mu a_\nu - \partial_\nu a_\mu)$ field.

c) *Three stress fields in fluid-flow fields*

There are three types of stress fields within the fluid flows: (A) *isotropic* stress field $\sigma_1^{jk}(x^\nu)$ (non-dissipative), (B) *anisotropic* stress $\sigma_A^{jk}(x^\nu)$ (non-dissipative), and (C) *viscous* stress $\sigma_{\text{vis}}^{jk}(x^k)$ (anisotropic and dissipative). As mentioned previously, the traditional Eulerian fluid system is governed by the isotropic pressure stress σ_1^{jk} . According to the FGT theory, on the other hand, the corresponding case of isotropic pressure stress σ_1^{jk} is accompanied by a transparent gauge field which is derived from a scalar potential $\Psi(x^\mu)$ (i.e. $a_\nu = \partial_\nu \Psi$).

Depending on whether the stress field is σ_1^{jk} (isotropic) or σ_A^{jk} (anisotropic), the fluid current field $j^\mu(x^\mu)$ changes its character drastically. In the latter case, the gauge field $a_\nu(x^\mu)$ takes intrinsic 4-vector form yielding non-vanishing $f_{\mu\nu}(= \partial_\mu a_\nu - \partial_\nu a_\mu)$. The third viscous stress σ_{vis}^{jk} plays an important role in the traditional Navier-Stokes system. Below, we look into the three stress fields in details.

(1) *Isotropic stress field σ_1^{jk} and transparent gauge field $\partial_\nu \Psi$*

If $a_\nu = \partial_\nu \Psi$, the field tensor $f_{\mu\nu}$ defined by (10) takes the form, $f_{\mu\nu} = \partial_\mu \partial_\nu \Psi - \partial_\nu \partial_\mu \Psi$. Hence $f_{\mu\nu} \equiv 0$. Then, the third Lagrangian \mathcal{L}_a vanishes identically, while the action principle applied to the remaining pair of Lagrangians ($\mathcal{L}_{\text{fluid}}, \mathcal{L}_{\text{int}}$) yield the equation (12) of the Eulerian fluid system since its derivation was independent of \mathcal{L}_a . The equation (12) under $f^{\mu\nu} = 0$ reduces to

$$\rho D_t v^k = \partial_j \sigma_1^{jk}, \quad \sigma_1^{jk} = -p \delta^{jk}, \quad j, k = 1, 2, 3. \quad (18)$$

This is the same as (4).⁶

The equation (13) must be discarded here because both of \mathcal{L}_a and $f_{\mu\nu}$ vanishes. However, a wonderful feature of this gauge theory is that the mass conservation equation is still deduced from the action principle under $a_\nu = \partial_\nu \Psi$. Varying the field $\Psi \rightarrow \Psi + \delta\Psi$ in \mathcal{L}_{int} of (8) with assuming the fluid current j^ν fixed, the action variation is given by $\delta S^{\text{FGT}} = c^{-1} \int j^\nu \partial_\nu (\delta\Psi) d\Omega$, which is transformed as

$$\delta S^{\text{FGT}} = -c^{-1} \int \partial_\nu j^\nu \delta\Psi d\Omega + \int \partial_\nu (j^\nu \delta\Psi) d\Omega. \quad (19)$$

The second is integrated once, leading to vanishing boundary integrals. Requiring $\delta S^{\text{FGT}} = 0$ for arbitrary $\delta\Psi$ results in (from (19)):

$$\partial_\nu j^\nu = \partial_t \rho + \nabla \cdot (\rho \mathbf{v}) = 0. \quad (20)$$

Thus, it is found in the particular case $a_\nu = \partial_\nu \Psi$ that the fluid system, described by the action S^{FGT} , reduces to the *Eulerian system* described by the Euler's equation of motion (18) and the continuity equation (20). The gauge field $a_\nu = \partial_\nu \Psi$ exists, but not observable. This may be said that the gauge field is *transparent*.

(2) *Anisotropic stress field σ_A^{jk} and colored gauge field a_ν*

Suppose that the gauge field a_ν makes a transition from the *transparent* field $\partial_\nu \Psi$ to general vector-potential a_ν yielding colored non-vanishing $f_{\mu\nu}$.⁷ Its experimental evidence

⁶ With the metric tensor $\delta_{jk} = \delta^{jk} = \text{diag}(1, 1, 1)$, we have $\sigma_{jk} = \eta_{ja} \eta_{kb} \sigma^{ab} = \sigma^{jk}$.

⁷ The "colored" is equivalent to " $f_{\mu\nu}$ non-vanishing". Non-dissipative anisotropic stress σ_A^{jk} was introduced first by [18]. Detailed analysis was done by [19] from *fluid-dynamics* view-point. Reinterpretation was given by [20] from the *gauge invariance*.

was given in the section III. This causes corresponding transition of stress tensor σ^{jk} within the flow field from the isotropic stress $\sigma_1^{jk} = -p\delta^{jk}$ to a new stress field with additional anisotropic part σ_A^{jk} . Rewriting the second force term on the right of (12) as $\rho f^{k\nu} v_\nu = \partial_\nu \sigma_A^{\nu k}$, the equation becomes

$$\rho D_t v^k = \partial_\nu \sigma_1^{\nu k} + \partial_\nu \sigma_A^{\nu k}, \quad (21)$$

where

$$\sigma_A^{jk} = e^j d^k + b^j h^k - w_e \delta^{jk}, \quad w_e \equiv \frac{1}{2} (\mathbf{e}, \mathbf{d}) + \frac{1}{2} (\mathbf{h}, \mathbf{b}) \quad (22)$$

$$\sigma_A^{00} = -w_e, \quad \sigma_A^{0k} = -c(\mathbf{d} \times \mathbf{b})^k, \quad (23)$$

for $j, k = 1, 2, 3$ and $\nu = 0, 1, 2, 3$. Definitions of \mathbf{d} and \mathbf{h} are given in the paragraph above (16). Using (22) and (23), the second force term $\partial_\nu \sigma_A^{\nu k}$ can be given another expression:

$$\partial_\nu \sigma_A^{\nu k} = \rho (\mathbf{f}_L)^k, \quad \mathbf{f}_L \equiv \mathbf{e} + \mathbf{v} \times \mathbf{b}, \quad (24)$$

This may be termed as *fluid-Lorentz force*, and the stress tensor $\sigma_A^{\nu k}$ is analogous to the Maxwell stress of Electromagnetism.

The anisotropic stress field $\sigma_A^{\nu k}$ was introduced in [13]. In the current fluid mechanics, the stress $\sigma_A^{\nu k}$ is still out of consideration. As a matter of fact, the viscous stress tensor σ_{vis}^{jk} , considered in the next item (3), is used in the current theory of fluid mechanics. The viscous stress tensor has anisotropic components as well. At the times of 1953 and 1967 when George Batchelor published his textbooks ([9], [10]), the anisotropic components of viscous stress might be useful in his study of fluid-dynamics and turbulence (see (3) below).

However, there exists an essential difference between the two fields of the viscous stress σ_{vis}^{jk} and the FGT stress $\sigma_A^{\nu k}$. The former is dissipative as shown in (3), while the latter is conservative because the mechanical systems derived from the action principle in terms of Lagrangians (like those of the sections a) and b) of § IV) have Hamiltonian system of equations of motion which conserve the total mechanical energy. Hence the present study emphasizes the importance of the field $\sigma_A^{\nu k}$.

(3) Viscous stress tensor σ_{vis}^{jk} and boundary layers

Concerning the expression $\sigma_1^{jk} = -p\delta^{jk}$, George Batchelor (the author of the book [10]) describes in its §3.3: "There is no reason to expect these results to be valid for a fluid in motion". The author's point is that the law $\sigma_1^{jk} = -p\delta^{jk}$ is valid in a fluid at rest. He continues: "The simple notion of a pressure acting equally in all directions is lost in most cases of a fluid in motion." And, "Tangential stresses are non-zero in general." The pressure is defined originally by the thermodynamics and the thermodynamic equations of state refer to equilibrium conditions, whereas the state of a fluid in motion are not in exact thermodynamic equilibrium.

It is convenient to regard the stress tensor σ_{ij} as the sum of an isotropic part $-p\delta_{ij}$ and a remaining non-isotropic part d_{ij} :

$$\sigma_{ij} = -p\delta_{ij} + d_{ij}, \quad (25)$$

where, assuming $d_{ii} = 0$, we have $p = -\frac{1}{3} \sigma_{ii}$, and the non-isotropic part d_{ij} may be termed the *deviatoric stress tensor*. Here the $p = -\frac{1}{3} \sigma_{ii}$ has a mechanical significance, generalizing the elementary notion of pressure, but reducing to the fluid pressure when the fluid is at rest.

Traditional fluid mechanics assumes that the deviatoric stress d_{ij} is originated by non-uniformity of the flow field, and seeks a linear local relation between the stress d_{ij} and local velocity gradients $\partial u_j/\partial x_i$. It is a usual custom to rewrite the velocity gradient $\partial u_j/\partial x_i = \partial_i u_j$ as

$$\partial_i u_j = e_{ij} + \xi_{ij}, \quad e_{ij} = \frac{1}{2} (\partial_i u_j + \partial_j u_i), \quad (26)$$

$$\xi_{ij} = \frac{1}{2} (\partial_i u_j - \partial_j u_i) = \frac{1}{2} \varepsilon_{ijk} \omega_k, \quad \omega_k = \varepsilon_{kij} \partial_i u_j, \quad (27)$$

where ε_{kij} is the alternating tensor⁸. According to the detailed tensor analysis (in §3.3 of [10], deleting contribution from the term ξ_{ij} after all), the deviatoric stress is given by

$$d_{ij} = 2\eta (e_{ij} - \frac{1}{3} \Delta \delta_{ij}), \quad \Delta \equiv e_{kk} = \text{div } \mathbf{u}, \quad (28)$$

satisfying $d_{ii} = 0$, where η is a viscosity coefficient. Thus, we find⁹

$$\sigma_{\text{vis}}^{jk} = 2\eta (e_{jk} - \frac{1}{3} \Delta \delta_{jk}). \quad (29)$$

Then the equation of motion is given by the form of well-known Navier-Stokes equation:

$$\rho D_t v^k = -\partial_k p + \partial_j \sigma_{\text{vis}}^{jk}. \quad (30)$$

In a special case where the divergence $\Delta = \text{div } \mathbf{v}$ is not significant, the above Navier-Stokes equation takes the following form

$$\rho = \rho_0 + \rho', \quad p = p_0 + p', \quad p' = c_s^2 \rho', \quad (31)$$

$$\rho \partial_t u_k + \rho u_j \partial_j u_k = -\partial_k p + \eta \nabla^2 u_k. \quad (32)$$

$$\rho u_j \partial_j u_k \approx \partial_j (\rho_0 u_j u_k) = \partial_j R_{jk}, \quad R_{jk} = \rho_0 u_j u_k \quad (33)$$

where v^k and ρ are replaced approximately with u_k and a constant ρ_0 when $\Delta = \partial_k v^k \approx \partial_k u_k$ is not significant.

In order to find the energy dissipated into heat by the motion of a viscous fluid (or *equivalently*, the heat energy gained by the fluid internally), one must define the thermodynamic state of the fluid, which is characterized with the density ρ , pressure p , specific internal energy ε (per unit mass), specific entropy s and specific enthalpy h , and temperature T . There is a unidirectional transfer of mechanical energy by the viscosity to the internal energy ε , *i.e.* irreversible dissipation into heat.

According to the texts ([10], [12]), the amount of heat gained by unit volume of the fluid is given by the following expression (see Appendix A), which can be shown to be non-negative:

$$\sigma_{\text{vis}}^{jk} \partial_k v_j = 2\eta (e_{jk} - \frac{1}{3} \Delta \delta_{jk})(e_{jk} - \frac{1}{3} \Delta \delta_{jk}) \quad (\geq 0), \quad (34)$$

where the heat conduction effect owing to non-uniform temperature ($\nabla T \neq 0$) is omitted. [*cf.* §3.4 of [10] or §49 of [12]. The latter text shows additional non-negative $\zeta \Delta^2$ to (34) from ζ .]

⁸ $\varepsilon_{ijk} = 0$ unless i, j, k are all different, with its value +1 or -1 according as i, j, k in cyclic order or not.

⁹ The textbook [12] adds one more term with the second (bulk) viscosity ζ : $\zeta \Delta \delta_{jk}$ stemming from the finite time response of molecular processes. Note that there is no distinction whether the indices are upper or lower in the present. See the note below (18).

V. STEADY STREAMING BY POWERFUL EXCITATION

Suppose that the acoustic waves in a closed tube were initially weak. The system is governed by the Eulerian system, but accompanying a transparent (invisible) gauge field $\partial_\nu \Psi$ (described in § III. B). As the wave intensity increases, the gauge field shows its appearance spontaneously at a transition when the field is colored with general rotational field superimposed on the transparent field. This is consistent with the Fluid Gauge Theory, which predicts the trace of background gauge field visualized by the Kundt's dust striations.

Furthermore, if there is a prolonged powerful acoustic excitation, *steady streaming* is generated within the tube filled with standing waves. A number of experimental photographs showing the steady streaming were presented by Andrade [6], which were observed under powerful excitation (FIG.5). The steady streaming is generated by the combined action of the nonlinear Reynolds stress and the viscous shear effect causing acoustic energy dissipation (see (38) given below). [cf. § 4.7 of [11]]. Lowering the intensity, but still above a critical intensity, he observed ripple-like striations.

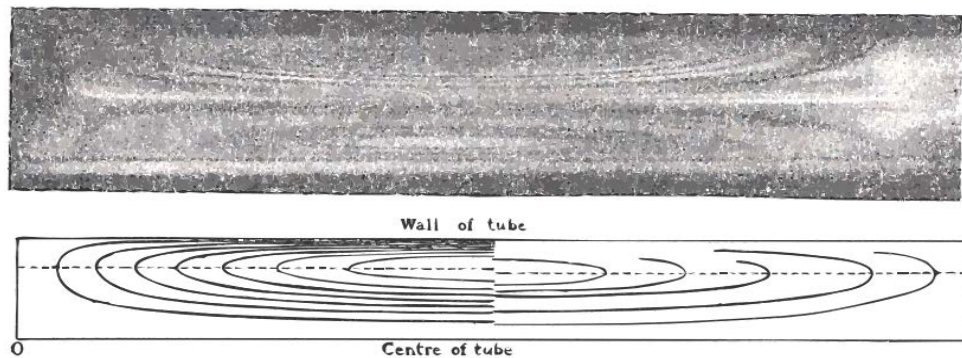


Fig. 5: Steady streamings of a single quarter-wave-length circulation in the Kundt tube experiment, shown by (a) Photograph (upper) taken for 600Hz sound resonance visualized with smoke by Andrade (FIG.13 of [6]), and (b) Streamlines (lower) between a pair of a node (left) and antinode (right): the curves on the right-hand half side were reproduced by reading the drift motion of smoke particles, while the curves on the left-hand half side are theoretical streamlines computed from Rayleigh's formula (FIG.5 of [6] and Ryleigh formula shown at pgae 453).

Citing the descriptions in the well-known classics [4] in 1890s, Rayleigh wrote his philosophical view on the acoustic problem initiated by Kundt [1] in §352 of [4]: "One of the most curious consequences of viscosity is the generation in certain cases of regular vortices. [Of this an example, discovered by Dvorak [3], has already been mentioned in §260.] In a theoretically inviscid fluid, no such effect could occur (§240); and, even when viscosity enters, the phenomenon is one of the second order, dependent, that is, upon the square of the motion."

Suppose that oscillations of the acoustic pressure are expressed as $p(t, x) = e^{i\omega t} f(x)$ in a closed tube. Resonant sound waves in the tube generate a steady streaming motion there. Such effect can occur by the action of Reynolds stress $\overline{\rho u_j u_k}$ when the acoustic energy dissipation takes place in thin boundary layers on the tube walls, where the overline signifies an average over a wave period, *i.e.* a mean value. The mean force \overline{F}_k with which waves act on a fluid element results from the gradient of Reynolds stress $\overline{R}_{jk} = \rho_0 \overline{u_j u_k}$, represented by $\overline{F}_k = -\partial_j(\rho_0 \overline{u_j u_k})$ from (33). Taking time average of (32) in the main part of sound waves (*i.e.* external to the viscous boundary layer) where the viscous effect of σ_{jk}^{vis} is not significant, one obtains the mean equation of motion:

$$\rho_0 \partial_t \bar{u}_k = \bar{F}_k - \partial_k \bar{p},$$

which reduces to $\bar{F}_k - \partial_k \bar{p} = 0$ since $\partial_t \bar{u}_k$ vanishes by the time derivative. Thus, we obtain the mean equation valid in the main part external to thin viscous boundary layers:

$$\partial_k \bar{p} = \bar{F}_k, \quad \bar{F}_x = -\partial_j \bar{R}_{jx} = -\partial_x(\rho_0 \bar{u}\bar{u}) - \partial_y(\rho_0 \bar{u}\bar{v}), \quad (35)$$

where $\bar{R}_{jk} = \rho_0 \bar{u}_j \bar{u}_k$. In this main wave part, there is balance of the two mean effects (gradients) of the pressure and the Reynolds stress. This implies the place where there is a driving force of the steady streaming. In fact, *departure* of the mean force $\partial_j \bar{R}_{jk}$ within the thin boundary layer from its external value $\partial_j (\bar{R}_{jk})_{\text{ex}} = \partial_j (\rho_0 \bar{u}_j \bar{u}_k)_{\text{ex}}$ generates streaming, because the external mean pressure \bar{p}_{ex} is unchanged, *i.e.* uniform approximately across thin boundary layer (see, *e.g.* §5.7 of [10]).

Hence the external mean pressure gradient $\partial_x \bar{p}_{\text{ex}}$ is given by \bar{F}_x of (35). rewritten as

$$\partial_x \bar{p}_{\text{ex}} = (\bar{F}_x)_{\text{ex}} = -\partial_j (\bar{R}_{jx})_{\text{ex}} = -\partial_x (\rho_0 \bar{u}\bar{u})_{\text{ex}} - \partial_y (\rho_0 \bar{u}\bar{v})_{\text{ex}}, \quad (36)$$

Within the boundary layer, the mean force \bar{F}_x is given by the negative of $\partial_j \bar{R}_{jx}$ where $\bar{R}_{xx} = \rho_0 \bar{u}^2$ and $\bar{R}_{yx} = \bar{R}_{xy} = \rho_0 \bar{u}\bar{v}$, which depart from those with the lower suffix "ex".¹⁰

A steady streaming \bar{u}^{st} is generated by the viscous shear force $\partial_y \sigma_{yx}^{\text{vis}} \approx \eta \partial_y^2 \bar{u}^{\text{st}}$ being in balance with two other forces, *i.e.* (i) gradient of mean Reynolds stress $\partial_j \bar{R}_{jx}$ and (ii) that of mean external pressure $\partial_x \bar{p}_{\text{ex}}$:

$$\eta \partial_y^2 \bar{u}^{\text{st}} - \partial_j \bar{R}_{jx} - \partial_x \bar{p}_{\text{ex}} = 0. \quad (37)$$

Substituting the expression for $\partial_x \bar{p}_{\text{ex}}$ of (36) and using the definition of $\partial_j \bar{R}_{jx}$, one can rewrite it as

$$\nu \partial_y^2 \bar{u}^{\text{st}} = (\partial_x \bar{u}^2 - \partial_x (\bar{u}^2)_{\text{ex}}) + (\partial_y (\bar{u}\bar{v}) - \partial_y (\bar{u}\bar{v})_{\text{ex}}), \quad (38)$$

where $\nu \equiv \eta/\rho_0$. To evaluate the 2nd order terms on the right hand side of (38), the expressions of u and v must be found from the linear theory of oscillatory boundary layers in the tube. It is reminded that the equations for the mean stream has been derived from the full nonlinear equations (32) and (33).

The mean equation (38) is linear with respect to the variable \bar{u}^{st} on the left hand side, so that one can represent it as a linear combination $\bar{u}^{\text{st}} = (\bar{u}^{\text{st}})_{uu} + (\bar{u}^{\text{st}})_{uv}$, each of which satisfies the following equations:

$$\nu \partial_y^2 (\bar{u}^{\text{st}})_{uu} = \partial_x \bar{u}^2 - \partial_x (\bar{u}^2)_{\text{ex}} \quad (39)$$

$$\nu \partial_y^2 (\bar{u}^{\text{st}})_{uv} = \partial_y (\bar{u}\bar{v}) - \partial_y (\bar{u}\bar{v})_{\text{ex}} \quad (40)$$

The linear theory of *Oscillatory Boundary Layers* is presented in the Appendix B. The axial x -velocity $u(t, x, y,)$ is given by (B16) of the Appendix B 3 as

¹⁰ The mean streaming \bar{u}^{st} is generated by departure of \bar{R}_{jx} from the external values $(\bar{R}_{jx})_{\text{ex}}$, which is in balance with the external pressure gradient \bar{p}_{ex} , keeping uniform across the thin boundary layer.

$$u(t, x, y,) = u_{\text{ex}}(x) \Re[\tilde{P}(t) F_{\kappa}(y)], \quad \tilde{P}(t) \equiv e^{i\omega t}. \tag{41}$$

$$F_{\kappa}(y) \equiv 1 - \exp \{-(i\omega/\nu)^{1/2} y\} = 1 - \exp \{-(1+i) \kappa y\}, \tag{42}$$

$$u_{\text{ex}}(x) \equiv U_0 \cos kx, \tag{43}$$

from the linear theory of the acoustic resonance under the oscillatory pressure gradient $P \equiv -\partial p_e/\partial x = u_{\text{ex}}(x)\Re[P_0 e^{i\omega t}]$, where $P_0 = \rho_0 i\omega$, $\kappa \equiv \sqrt{\omega/2\nu}$, and $u_{\text{ex}}(x)$ is a real function of x . Note that $(i\omega/\nu)^{1/2} y = (1+i) \kappa y$.

From this u -solution, the y -component $v(t, x, y,)$ is found as

$$v(t, x, y,) = u'_{\text{ex}}(x) \Re [(\nu/(i\omega))^{1/2} \tilde{P}(t) F_{\kappa}(y)], \tag{44}$$

where $u'_{\text{ex}}(x) = du_{\text{ex}}/dx$. (cf. Eq. (205) and (206) of Chap.4 of [11]).

It is shown in the linear theory of Appendix ?? that the above expressions of u and v satisfy the linearized equation of continuity: $\partial_t \rho_{\text{ex}} + \rho_0(\partial_x u + \partial_y v) = 0$. From (41) and (44), one can find time-averages of the wo products \overline{uv} and $\overline{u^2}$ to be used for (39) and (40).

First, we consider \overline{uv} and the equation (40). Taking a product of the real parts of (41) and (44), one obtains after taking its time average:

$$\overline{uv} = \frac{1}{2} (\nu/2\omega)^{1/2} u_{\text{ex}}(x) u'_{\text{ex}}(x) \left| F_{\kappa}(y) \right|^2, \tag{45}$$

and its external value is $(\overline{uv})_{\text{ex}} = \frac{1}{2} (\nu/2\omega)^{1/2} u_{\text{ex}}(x) u'_{\text{ex}}(x)$ as $\kappa y \rightarrow \infty$. Integrating (40) with y twice, the mean streaming $\overline{u_{uv}^{\text{st}}}$ generated by the departure of \overline{uv} from the external value in the oscillating boundary layer is given by

$$\begin{aligned} \overline{u_{uv}^{\text{st}}} &= \nu^{-1} \int_0^y [\overline{uv} - (\overline{uv})_{\text{ex}}] dy \\ &= \nu^{-1} \frac{1}{2} \frac{\nu}{\omega} \frac{1}{\sqrt{2}} u_{\text{ex}}(x) u'_{\text{ex}}(x) \int_0^y \left[\left| F_{\kappa}(y) \right|^2 - 1 \right] d(\kappa y), \end{aligned} \tag{46}$$

where $\kappa \equiv \sqrt{\omega/2\nu}$. At the external edge of the boundary layer as $\zeta \equiv \kappa y$ tends to ∞ , the integral in the last expression can be estimated as

$$\int_0^{\zeta} \left[\left| 1 - \exp \{-(1+i) \zeta_*\} \right|^2 - 1 \right] d\zeta_* \rightarrow -1/\sqrt{2} \quad (\text{as } \zeta \rightarrow \infty).$$

Hence, the steady streaming generated by \overline{uv} at the edge external to the boundary layer is

$$\overline{u_{uv}^{\text{st}}} = -\frac{1}{4\omega} u_{\text{ex}}(x) u'_{\text{ex}}(x) \tag{47}$$

¹¹ $\overline{u^2} = \frac{1}{2} (u_{\text{ex}})^2 |F_{\kappa}|^2$ and $|F_{\kappa}|^2 = 1 - 2e^{-\kappa y} \cos \kappa y + e^{-2\kappa y}$. This is because $u^2 = (u_{\text{ex}})^2 \Re[\tilde{P}(t) F_{\kappa}(y)]^2 = \Re[e^{i\omega t} F_{\kappa}(y)]^2 = (1/4)(u_{\text{ex}})^2 (e^{i\omega t} F_{\kappa} + e^{-i\omega t} \hat{F}_{\kappa})^2 = (1/4) (e^{2i\omega t} F_{\kappa}^2 + e^{-2i\omega t} \hat{F}_{\kappa}^2 + 2|e^{i\omega t}| |F_{\kappa}|^2)$ where \hat{F}_{κ} is the complex conjugate of F_{κ} . Taking time average $\langle \cdot \rangle_{\text{av}}$, we have $\langle e^{\pm 2i\omega t} \rangle_{\text{av}} = 0$ and $\langle |e^{i\omega t}| \rangle = 1$. $\partial_x \overline{p_{uu}} = -(1/4)u_{\text{ex}}^2 \delta$, $\delta = 1/\kappa$

Secondly, there is one more contribution from the component \overline{uu} of Reynolds stress. The steady stream $(\overline{u^{st}})_{uu}$ generated by \overline{uu} is found from the equation (39). Taking a double product of the real part of u given by (41), one obtains after taking its time average:¹¹

$$\overline{uu} = \frac{1}{2} u_{\text{ex}}^2 |F_{\kappa}(y)|^2 \quad (48)$$

and its external value is $(\overline{uu})_{\text{ex}} = \frac{1}{2} u_{\text{ex}}^2$ since $|F_{\kappa}(y)|^2 \rightarrow 1$ as $\kappa y \rightarrow \infty$. Substituting these values of \overline{uu} and $(\overline{uu})_{\text{ex}}$ to the right hand side of (39) and integrating with respect to y , we have

$$\nu \partial_y (\overline{u^{st}})_{uu} = \frac{1}{2\kappa} (du_{\text{ex}}^2(x)/dx) \int_0^{\zeta} [-2e^{-\zeta} \cos \zeta + e^{-2\zeta}] d\zeta - \rho_0^{-1} \partial_x \overline{p}_{uu}. \quad (49)$$

where the last term $-\rho_0^{-1} \partial_x \overline{p}_{uu}$ is a function of x only, which is arbitrary in general, but its functional form is fixed by the argument just below.

Requiring the influence of viscous friction force vanishing externally from the boundary layer, $\nu \partial_y (\overline{u^{st}})_{uu} \rightarrow 0$ as $\zeta = \kappa y \rightarrow \infty$, the counter pressure force $-\rho_0^{-1} \partial_x (\overline{p}_{uu})_{\text{ex}}$ owing to the Reynolds stress \overline{uu} must be given by $(1/4\kappa)(du_{\text{ex}}^2(x)/dx)$ at the edge of the boundary layer. Then, deleting the counter pressure force, we have

$$\nu \partial_y (\overline{u^{st}})_{uu} = \frac{1}{2\kappa} u_{\text{ex}} u'_{\text{ex}} [-e^{-2\zeta} + 2e^{-\zeta}(\cos \zeta - \sin \zeta)]. \quad (50)$$

Integrating this with respect to ζ for entire range $[0, \infty]$, we obtain the steady streaming generated by \overline{uu} at the edge external to the boundary layer:

$$(\overline{u^{st}})_{uu} = \nu^{-1} \frac{1}{2} \frac{1}{\kappa^2} u_{\text{ex}} u'_{\text{ex}} \left(-\frac{1}{2}\right) = -\frac{1}{2\omega} u_{\text{ex}}(x) u'_{\text{ex}}(x). \quad (51)$$

since $1/\kappa^2 = 2\nu/\omega$. Summing up this term $(\overline{u^{st}})_{uu}$ with $(\overline{u^{st}})_{uv}$ of (47), we find finally the total value:

$$(\overline{u^{st}})_{\text{total}} = (\overline{u^{st}})_{uu} + (\overline{u^{st}})_{uv} = -\frac{3}{4} \frac{1}{\omega} u_{\text{ex}}(x) u'_{\text{ex}}(x). \quad (52)$$

(cf. Eq. (215) of Chap.4 of [11]).

VI. SPONTANEOUS SYMMETRY TRANSITIONS: KUNDT'S SYSTEM AND HIGGS' MECHANISM

An analogy exists in the Lagrangian structures in two physical systems between Kundt's symmetry transition and Higgs' mechanism. Let us consider the Higgs' mechanism from the *abelian gauge theory* [21, 22]. Suppose that a massive charged scalar field $\phi (= \phi_1 + i\phi_2)$ is interacting with an electromagnetic field A_{μ} (a massless vector boson). Its Lagrangian is given by $\mathcal{L} = \mathcal{L}_{\phi} + \mathcal{L}_A$:

$$\mathcal{L}_\phi = (D^\mu \phi)^* D_\mu \phi - \mu^2 \phi^* \phi - \lambda (\phi^* \phi)^2, \quad D_\mu \equiv \partial_\mu - ieA_\mu, \quad (53)$$

$$\mathcal{L}_A = -(1/4) F_{\mu\nu} F^{\mu\nu}, \quad F_{\mu\nu} = \partial_\mu A_\nu - \partial_\nu A_\mu, \quad (54)$$

where e is the electric charge, $\lambda (> 0)$ being a constant parameter, and another parameter μ^2 taking positive or negative values (according to the tradition of field theory). The Lagrangian \mathcal{L}_ϕ is invariant under the local U(1) transformation.

For $\mu^2 > 0$, the Lagrangian describes physics of a massless gauge field A_μ coupled with a complex scalar field ϕ of mass μ with ϕ^4 self-interaction. This corresponds to the case of our transparent gauge field considered in § IV c) (1), where the *transparent gauge field* corresponds to the *massless gauge boson* in this analogy, while the *particle field* ϕ corresponds to *fluid current field*.

For $\mu^2 < 0$, the field will acquire a vacuum expectation value $\phi_0 = \langle \phi \rangle_0 = v/\sqrt{2}$ ($v^2 = -\mu^2/\lambda > 0$), and new symmetries emerge. As traditional, let us take the minimum ϕ_0 along the direction of the real part of ϕ and expand the ϕ -field in its vicinity: $\phi(x) = (1/\sqrt{2})(v + \phi_1(x) + i\phi_2(x))$. Substituting this form, the Lagrangian $\mathcal{L} = \mathcal{L}_A + \mathcal{L}_\phi$ can be rearranged as $\mathcal{L} \equiv \mathcal{L}^{\text{Higgs}} = \mathcal{L}_\phi^{(m)} + \mathcal{L}_{\text{intG}} + \mathcal{L}_A^{(m)}$, where

$$\mathcal{L}_\phi^{(m)} = \frac{1}{2} (\partial_\mu \phi_1)^2 + \frac{1}{2} (\partial_\mu \phi_2)^2 - \frac{1}{2} m_\phi^2 \phi_1^2, \quad (55)$$

$$\mathcal{L}_{\text{intG}} = m_A A_\mu \partial^\mu \phi_2 \quad (\text{a Goldstone-mode term}), \quad (56)$$

$$\mathcal{L}_A^{(m)} = -(1/4) F_{\mu\nu} F^{\mu\nu} + \frac{1}{2} m_A^2 A_\mu A^\mu, \quad (57)$$

where $m_\phi^2 = 2v^2\lambda$ and $m_A = ev$. The third $\mathcal{L}_A^{(m)}$ describes the gauge field A_μ which acquired a mass term proportional to m_A^2 . One can see similarity of the above triplet of Lagrangians, $[\mathcal{L}_\phi^{(m)}, \mathcal{L}_{\text{intG}}, \mathcal{L}_A^{(m)}]$ in each form with the triplet of FGT Lagrangians, $[\mathcal{L}_{\text{fluid}}, \mathcal{L}_{\text{int}}, \mathcal{L}_a]$ given by (7), (8) and (9).

Most obvious similarity is seen in the forms of $\mathcal{L}_{\text{intG}}$ of (56) and $\mathcal{L}_{\text{int}} = c^{-1} j^\nu a_\nu$ of (8), comparing those from the viewpoint of the *de Broglie* concept for the momentum associated with $\partial^\mu \phi_2$ of (56), in which the factor $A_\mu \partial^\mu \phi_2$ is analogous to $a_\nu j^\nu$ of \mathcal{L}_{int} . Next, the first member $\mathcal{L}_\phi^{(m)}$ describes the massive scalar particle field ϕ , while its FGT counterpart $\mathcal{L}_{\text{fluid}}$ describes the massive fluid current.

In the beginning, the Lagrangian \mathcal{L}_A described the massless gauge boson, which has been transformed to $\mathcal{L}_A^{(m)}$ having a mass term $\frac{1}{2} m_A^2 A_\mu A^\mu$ after the transition. Corresponding FGT Lagrangian is \mathcal{L}_a of (9), and the FGT gauge field a_ν is governed by the equation (13): $\partial_\lambda f^{\nu\lambda} = \mu j^\nu$. Obviously, the field tensor $f^{\nu\lambda}$ is controlled and *colored* by the fluid current j^ν giving an inertial effect (*i.e.* an inertial influence) on the evolution of the gauge field a_ν .

VII. SUMMARY

In the Kundt tube experiment [1], an interesting anomaly is known, *i.e.* there existed two characteristic scales observed in the experiment. One is the wave-length λ_r of the sound

wave in resonance within the tube, and the other is the dust striations formed in the resonant standing wave characterized with much shorter longitudinal scales ℓ . Formation mechanism of the second dust striations has remained unresolved for a long time.

Fluid Gauge Theory has been proposed to explain the formation mechanism of the dust striation. The new fluid theory is based on the concepts of the gauge theories in Physics. Although certain fluid motions are described by both of the traditional Eulerian equations and the new Fluid Gauge Theory, there is a difference between the two. The flow field of the FGT theory is now accompanied by a gauge field behind it. In this case, the pressure stress field is *isotropic*, the gauge field is transparent and the flow field is mainly irrotational. However, the invisible gauge field acts to guarantee the law of mass conservation.

Fluid Gauge Theory [13] eventually allows transition of the isotropic pressure stress field existing in the Eulerian field to anisotropic stress field. Correspondingly, the flow field becomes rotational and the trace of gauge field is visualized by eddies. In this case too, the mass conservation is ensured by the action of the background gauge field. Owing of this, the FGT theory does not set the continuity equation *a priori* from the outset. Transition of the stress field from the isotropic to anisotropic occurs spontaneously. The transition from irrotational flow field to rotational one is often caused by the action of viscosity (existing in real fluids).

Fluid Gauge Theory can represent new mechanism of transverse rotational waves of a characteristic length scale ℓ , which coexists in the field of longitudinal irrotational acoustic waves in resonance of another scale λ_r . This is the case of the dust striation. Since the oscillation frequencies of both modes share the same excitation frequency, the difference of the two longitudinal scales might be associated with the difference of respective phase velocity: one is c_s (the sound velocity of irrotational waves) and the other c_g (the velocity of rotational waves of gauge field). Thus, we have $\ell/\lambda_r = c_g/c_s$. Before the transition, there existed only the longitudinal irrotational acoustic waves. This is understood as a symmetry transition in the acoustic system according to the Fluid Gauge Theory. The larger acoustic scale of the resonance mode is that described by the Eulerian system. The second new smaller scales are generated by rotational eddy modes, predicted by the Fluid Gauge Theory.

It is surprising that the Lagrangian representation of the Fluid Gauge Theory has disclosed the similarity of two phenomena observed in quite different physical fields: one is the spontaneous formation of dust striation in the Kundt's acoustic experiment and the other the Higgs Mechanism of the particle physics. It is a quite unexpected finding that an analogy exists between the Lagrangian structures of both systems: Kundt and Higgs. Each system is described by a triplet of Lagrangians, each of which has similarity respectively. Most obvious similarity is seen in the forms of the Lagrangian describing interactions (see § VI).

When there is a prolonged powerful acoustic excitation, *steady streaming* is generated within the tube filled with standing waves. The steady streaming is generated by the combined action of the nonlinear Reynolds stress and the viscous shear effect. Andrade [6] presented experimental photographs showing this steady streaming. However, this was observed under prolonged intensive sound waves. Lowering the intensity, but still above a critical intensity, he observed ripple-like striation with using minute cork particles.

Finally, it is emphasized the *dust striation* is a visualized trace of a background rotational gauge field existing in the acoustic field of longitudinal irrotational waves. The formation mechanism of dust striation is understood as a spontaneous transition of symmetry in the acoustics, analogous to that known in the field theory.

APPENDIX

Appendix A: Energy equation and Entropy equation of a viscous fluid

Suppose a viscous fluid in motion with its thermodynamic state characterized with the density ρ , pressure p , specific internal energy ε , specific entropy s and specific enthalpy h (specific denoting per unit mass), and temperature T . The continuity equation (20) and the equation of motion (30) are

$$\partial_t \rho + \nabla \cdot (\rho \mathbf{v}) = 0, \quad \rho \partial_t v_k + \rho \mathbf{v} \cdot \nabla v_k = -\partial_k p + \partial_j \sigma_{\text{vis}}^{jk}. \quad (\text{A1})$$

The stress σ_{vis}^{jk} is rewritten as $\sigma_{jk}^{(\text{vis})}$ below.

Energy density (per unit volume) of the fluid in motion with velocity $\mathbf{v} = (v_k)$ is given by $E = \frac{1}{2} \rho v^2 + \rho \varepsilon$. Total energy flux F_k passing through unit area in a fluid per unit time to the x_k -direction is given by $F_k = \rho v_k (\frac{1}{2} v^2 + h) - v_j \sigma_{jk}^{(\text{vis})} - \kappa \partial_k T$ where κ is the thermal conductivity (from [12], §49). According to the general law of physics, the conservation of energy is expressed by $\partial_t E = -\partial_k F_k$. Namely, we have

$$\partial_t (\frac{1}{2} \rho v^2 + \rho \varepsilon) = -\partial_k (\rho v_k (\frac{1}{2} v^2 + h) - v_j \sigma_{jk}^{(\text{vis})}). \quad (\text{A2})$$

where the thermal conduction effect ($\kappa \partial_k T$) is omitted for simplicity because this section is concerned with only the mechanism of viscous dissipation of kinetic energy $\frac{1}{2} \rho v^2$ and associated increases of the internal energy ε and entropy s .

According to §49 of [12], using the continuity equation and equation of motion of (A1) helped by thermodynamic relations¹², the left-hand side of (A2) can be transformed to

$$\begin{aligned} \partial_t (\frac{1}{2} \rho v^2 + \rho \varepsilon) &= -\partial_k (\rho v_k (\frac{1}{2} v^2 + h) - v_j \sigma_{jk}^{(\text{vis})}) \\ &\quad + \rho T (\partial_t s + \mathbf{v} \cdot \nabla s) - \sigma_{jk}^{(\text{vis})} \partial_k v_j. \end{aligned} \quad (\text{A3})$$

Comparing both of the right-hand side of (A2) and (A3), the second line of (A3) must vanish. Hence we have the entropy equation,

$$\rho T (\partial_t s + \mathbf{v} \cdot \nabla s) = \sigma_{jk}^{(\text{vis})} \partial_k v_j, \quad (\text{A4})$$

in addition to the energy equation (A2). The quantity $\sigma_{jk}^{(\text{vis})} \partial_k v_j$ on the right-hand side is shown to be positive by (34) in the main text (§ IV. C. (3)).

The above result states that the total energy is conserved by the equation (A2) if the heat energy is taken into account, where the heat energy is transformed from the kinetic energy and an associated increase of the entropy s is given by the equation (A4) characterizing the thermodynamic state of the fluid.

Lastly, it would be instructive to consider that the last term $-v_j \sigma_{jk}^{(\text{vis})}$ on the right of (A2) is regarded as a energy flux (*i.e.* a rate of working) due to the viscosity action. Consider a

¹² Enthalpy: $h = \varepsilon + p/\rho$; Differentials of state variables: $d\varepsilon = T ds + (p/\rho^2) d\rho$; $\partial_t \varepsilon = T \partial_t s + (p/\rho^2) \partial_t \rho$, and $\partial_t \rho = -\partial_k (\rho v_k)$. Time derivatives: $\partial_t (\frac{1}{2} \rho v^2) = \rho v_k \partial_t v_k = \rho v_k (-v_k \partial_k v_k - v_k \partial_k p + v_k \partial_j \sigma_{jk}^{(\text{vis})})$, $\partial_t (\rho \varepsilon) = \rho \partial_t \varepsilon + \varepsilon \partial_t \rho = \rho T \partial_t s + h \partial_t \rho = \rho T \partial_t s - h \partial_k (\rho v_k)$. $\rho v_k \partial_k \varepsilon = \rho v_k T \partial_k s + (p/\rho) v_k \partial_k \rho$.

fluid volume \mathcal{V} surrounded by a closed surface \mathcal{S} . The rate at which a work W is done to outside fluid across the surface \mathcal{S} by the fluid in \mathcal{V} with the viscous stress $\sigma_{jk}^{(\text{vis})}$ is given by

$$\begin{aligned} W &= \int_{\mathcal{S}} v_j \sigma_{jk}^{(\text{vis})} n_k dS = \int_{\mathcal{V}} \partial_k (v_j \sigma_{jk}^{(\text{vis})}) dV = \int_{\mathcal{V}} \left[v_j \partial_k \sigma_{jk}^{(\text{vis})} + (\partial_k v_j) \sigma_{jk}^{(\text{vis})} \right] dV \\ &= \int_{\mathcal{V}} v_k F_k^{(\text{vis})} dV + \int_{\mathcal{V}} [(\partial_k v_j) \sigma_{jk}^{(\text{vis})}] dV, \quad F_k^{(\text{vis})} \equiv \partial_j \sigma_{jk}^{(\text{vis})}. \end{aligned} \quad (\text{A5})$$

where $\sigma_{jk}^{(\text{vis})} = \sigma_{kj}^{(\text{vis})}$, and n_k is unit outward normal to the enclosing surface \mathcal{S} . Since the work W is done to external fluid, the work to the fluid inside \mathcal{S} is $W_{\text{in}} = -W$. This implies the term $-v_j \sigma_{jk}^{(\text{vis})}$ denotes the work (an energy flux) within the fluid itself.

The integrand $v_k F_k^{(\text{vis})}$ in the first integral of (A5) denotes the mechanical work done by the viscous force $F_k^{(\text{vis})} = \partial_j \sigma_{jk}^{(\text{vis})}$ of (A1), while the integrand $(\partial_k v_j) \sigma_{jk}^{(\text{vis})}$ in the second integral denotes the energy dissipated into heat by the viscous action. The last is nothing but the expression of the right-hand side of (A4), confirming the consistence of the theory.

Appendix B: Oscillatory Boundary Layers

In order to see the difference and transition of the stress fields before and after certain spontaneous change, simple model analyses are presented in this Appendix B.

Let us consider a fluid in $2d$ (x, y) -channel with the channel axis to the x -direction and its width H to the normal y -direction. Not only the sound oscillation in the channel, but also other special conditions are imposed to consider analogous model problems. The fluid is supposed to be under pressure p_e , which is either uniform (with uniform fluid density ρ_0) in the first case B1, or subjected to a pressure gradient $P \equiv -\partial p_e / \partial x$ in the x -direction which is uniform spatially but oscillates sinusoidally in time $P(t)$ in the second case B2. Regarding the boundary conditions, the upper wall $y = H$ is kept at rest, while the lower wall $y = 0$ is in motion or at rest depending on each case. The fluid observes the no-slip condition on both walls.

In the third case B3, P is $P(t, x)$, periodic both temporally and spatially, and the fluid follows the no-slip condition on both walls at rest. Representative velocity u' of fluid flow is assumed very small compared to the sound speed c_s , and the density change $\Delta\rho$ is related to the pressure change Δp isentropically, with the specific entropy s being fixed:

$$\Delta p = c_s^2 \Delta\rho, \quad c_s^2 = \partial p / \partial \rho|_{s:\text{fixed}}. \quad (\text{B1})$$

The relative density change $\Delta\rho/\rho_0$ is small,¹³ of the order of 10^{-3} .

Before the transition, the motion is governed by the equation (18) under the isotropic pressure stress σ_1^{jk} . However in this model analysis, no-slip condition is applied on both of the upper and lower walls, so that the viscous stress term σ_{vis}^{jk} is included in the equation of motion. Furthermore, the fluid motion is assumed to take *unidirectional* velocity field, $\mathbf{v}_{\text{uni}} = (u(y, t), 0, 0)$, governed by the Navier-Stokes equation (30).

¹³ The equation (B2) can be written as $\rho \partial_t u \approx -\partial_x p_e$ out of thin viscous boundary layer. Using $\rho \partial_t u \approx \rho_0 i \omega u' = i \rho_0 k c_g u'$ and $\partial_x p_e = (\partial p_e / \partial \rho) \partial_x \rho \approx c_s^2 i k \rho'$. Then, $|\rho' / \rho_0| \approx |u' / c_s| (c_g / c_s) \approx 10^{-3}$.

For the unidirectional flow field \mathbf{v}_{uni} , the NS-eq.(30) reduces to

$$\rho \partial_t u = P + \rho \nu \partial_y^2 u, \quad P = -\partial p_e / \partial x, \quad \nu \equiv \eta / \rho. \quad (\text{B2})$$

Let us now consider the above three cases, step by step, in order to arrive at desired expressions, with improving boundary conditions imposed at the lower wall and with-and-without pressure oscillation.

1. Lower wall oscillates in its own plane while upper wall kept at rest

First, the lower wall makes a time periodic motion of a period T with its x -velocity U_w represented by the real part of $u_w e^{i\omega t}$ with $\omega = 2\pi/T$ the angular frequency:

$$U_w(t) = \Re[u_w e^{i\omega t}] = u_w \cos 2\pi(t/T), \quad (\text{B3})$$

where u_w is real and denotes the amplitude of wall oscillation. Namely the wall is moving in its own plane with a sinusoidal oscillation. The solution $u(y, t)$ satisfying (B2) is given by

$$u(y, t) = \Re \left[u_w e^{i\omega t} \frac{\sinh[K(1-Y)]}{\sinh K} \right]; \quad Y = \frac{y}{H}, \quad \frac{K}{H} = \left(\frac{i\omega}{\nu} \right)^{1/2} = \sqrt{\frac{\omega}{2\nu}}(1+i). \quad (\text{B4})$$

One can easily check that this satisfies not only the equation (B2) under $P = 0$, but the boundary conditions at $y = 0$ and H as well.

As $H \rightarrow \infty$, this tends to the solution found by Stokes:

$$u(y, t) \rightarrow \Re[u_w e^{i\omega t} \exp[-(i\omega/\nu)^{1/2} y]], \quad (\text{B5})$$

This solution represents an oscillating motion adjacent to the wall, called the *Stokes' oscillatory boundary layer* (see §4.3 of [10], or §4.7 of [11]). This is generated by the viscous dragging effect caused by the oscillating boundary wall at $y = 0$. The viscous dragging is expressed by the exponential factor:

$$\exp[-(i\omega/\nu)^{1/2} y] = \exp[-(\omega/2\nu)^{1/2} y] \cdot \exp[-i(\omega/2\nu)^{1/2} y]$$

since $\sqrt{i} = (1+i)/\sqrt{2}$. The effective thickness δ_{vis} of the viscous layer is found from the first factor $\exp[-(1/\delta_{\text{vis}}) y]$ where $\delta_{\text{vis}} = \sqrt{2\nu/\omega}$. The second factor $\exp[-i(y/\delta_{\text{vis}})]$, combined with the time factor $e^{i\omega t}$ of (B5), represents a wave propagating away from the wall: $\exp[i(\omega t - (y/\delta_{\text{vis}}))]$.

The thickness $\delta_{\text{vis}} = \sqrt{2\nu/\omega}$ is found very small, compared with an experimental channel width $H \approx 5 \text{ cm}$, if we take the experimental frequency $f = \omega/(2\pi)$ of the order 10^3 s^{-1} and the air kinematic viscosity $\nu_{\text{air}} = 0.15 \text{ cm}^2 \text{ s}^{-1}$ (at normal conditions): $\delta_{\text{vis}} \approx 10^{-2} \text{ cm}$, and $H/\delta_{\text{vis}} \approx 10^3$.

2. Time-periodic oscillation of pressure gradient with walls at rest

In the previous section B 1, the time periodic oscillation $e^{i\omega t}$ is imposed uniformly to the lower wall. Here, instead of the wall motion, a pressure oscillation is applied to the whole fluid (in the channel) uniformly with $P(t) = P_0 e^{i\omega t}$ at all points, with the static condition $U_w = 0$ applied at the wall boundaries.

First, we consider the case $H \rightarrow \infty$ and use the solution (B5) in order to find a solution of the present case. Far away from the lower wall ($y/\delta_{\text{vis}} \gg 1$), the viscous dragging effect by the no-slip condition at the wall $y = 0$ decays exponentially as y/δ_{vis} increases, and the equation (B2) tends to be approximated by $\rho \partial_t u = P(t)$. Assuming $u \propto e^{i\omega t}$, this is solved by $u_\infty = (\rho i \omega)^{-1} P(t)$, where $\partial_t u = i\omega u$ is used.

Regarding the full equation (B2), let us assume $u(y, t)$ having the time factor $e^{i\omega t}$ and write as $u(y, t) - u_\infty = u_\infty f(y)$ by using unknown function $f(y)$, the equation (B2) can be written as $(\rho i \omega) (u_\infty + u_\infty f(y)) = (\rho i \omega) u_\infty + \rho \nu u_\infty \partial_y^2 f$ with using $P = (\rho i \omega) u_\infty$. This reduces to an ordinary differential equation for $f(y)$:

$$f''(y) - (i\omega/\nu) f(y) = 0. \quad (\text{B6})$$

where the boundary conditions are: $f(0) = -1$ to satisfy $u(0, t) = 0$ and $f(\infty) = 0$ to satisfy $u(0, t) = u_\infty$. Thus, the solution $u(y, t)$ of (B2), tending to u_∞ as $y/\delta_{\text{vis}} \rightarrow \infty$, is given by

$$u(y, t) = \Re[(\rho i \omega)^{-1} P(t) [1 - \exp\{-(i\omega/\nu)^{1/2} y\}]], \quad P(t) = P_0 e^{i\omega t}. \quad (\text{B7})$$

This solution (B7) has been found for the infinite fluid layer with $H \rightarrow \infty$. However, in view of the estimate given in the last paragraph of B1 where $H/\delta_{\text{vis}} \approx 10^3$, one may use (B7) for a finite H with sufficient accuracy. This solution (B7) can be used practically as the $u(y, t)$ for the lower half $0 < y \leq \frac{1}{2} H$ of the channel under the oscillation pressure gradient P (simulating an acoustic oscillation),

3. Pressure oscillation both time-periodic and space-periodic

Here, in addition to the time periodic motion (of period T), a space-periodic structure (with a wavelength λ_g)¹⁴ is imposed for the pressure gradient $P \equiv -\partial p_e/\partial x$ to the x -direction, represented as¹⁵

$$P_+(t, x) = P_0 e^{i\omega t} e^{+ikx}, \quad \omega = 2\pi/T, \quad k = 2\pi/\lambda_g, \quad (\text{B8})$$

with the condition $U_w = 0$ applied at the wall boundaries. The solution $u(t, x, y)$ to

$$\rho \partial_t u = P_+ + \rho \nu \partial_y^2 u, \quad P_+ = -\partial p_e/\partial x, \quad (\text{B9})$$

(equivalent to (B2)), tending to $U_{\text{ex}}^\dagger(t, x)$ as $y/\delta_{\text{vis}} \rightarrow \infty$, is given by

$$u_+(t, x, y) = \Re[U_{\text{ex}}^\dagger(t, x) F(y)], \quad U_{\text{ex}}^\dagger(t, x) = (\rho i \omega)^{-1} P_+(t, x), \quad (\text{B10})$$

$$F(y) = 1 - \exp\{-(i\omega/\nu)^{1/2} y\}. \quad (\text{B11})$$

¹⁴ The wavelength λ_g is defined by $c_g T$, where c_g is the phase speed of the gauge field a_ν and T denotes the same period of sound vibration. For the sound speed $c_s = 344$ m/s (at 20° C), the sound wavelength λ_s is given by $c_s T$, and the following parameters are used: $c_g/c_s = \lambda_g/\lambda_s = 0.031$ and $u_w/c_g = 0.05$.

¹⁵ The suffices " + " or " † " denote the expressions derived from the x -space periodicity e^{+ikx} . This is to discriminate those derived from the e^{-ikx} periodicity to be given next.

Corresponding y -component $v_+(t, x, y)$ is given by

$$v_+(t, x, y) = \Re \left[(\nu/i\omega)^{1/2} (\partial U_{\text{ex}}^\dagger/\partial x) F(y) \right], \quad (\text{B12})$$

We can calculate $\partial_x u_+ + \partial_y v_+$, which is found as

$$\begin{aligned} \partial_x u_+ + \partial_y v_+ &= \Re \left[\partial_x U_{\text{ex}}^\dagger \left((1 - e^{-\kappa y}) + e^{-\kappa y} \right) \right] = \Re \left[\partial_x U_{\text{ex}}^\dagger \right] = \Re \left[-ik/(\rho i \omega) P_{\text{ex}}^\dagger \right] \\ &= \Re \left[- (1/\rho_0) i \omega \rho_{\text{ex}}^\dagger \right] = - (1/\rho_0) \partial_t \rho_{\text{ex}}^\dagger. \end{aligned} \quad (\text{B13})$$

since $P_{\text{ex}}^\dagger = -\partial_x p_{\text{ex}}^\dagger = ik(c_s^2 \rho_{\text{ex}}^\dagger) = i(\omega^2/k) \rho_{\text{ex}}^\dagger$ and $\omega = kc_s$. The last expression implies the following linearized continuity equation:

$$\partial_t \rho_{\text{ex}}^\dagger + \rho_0 (\partial_x u_+ + \partial_y v_+) = 0. \quad (\text{B14})$$

Next, under another pressure gradient given by $P_-(t, x) = P_0 e^{i\omega t} e^{-ikx}$, one can easily find the solution $u_-(t, x, y)$ with the parallel analysis, represented as

$$u_-(t, x, y) = \Re \left[U_{\text{ex}}^-(t, x) F(y) \right], \quad U_{\text{ex}}^-(t, x) = (\rho i \omega)^{-1} P_-(t, x), \quad (\text{B15})$$

Thus, we can give a representation of the external x -velocity in a resonant sound wave by the linear combination of $u_+(t, x, y)$ and $u_-(t, x, y)$:

$$\begin{aligned} u_{\text{res}}(t, x, y) &= u_+ + u_- = \Re \left[U_{\text{ex}}^\dagger(t, x) F(y) \right] + \Re \left[U_{\text{ex}}^-(t, x) F(y) \right] \\ &= \Re \left[u_{\text{ex}}(x) e^{i\omega t} F(y) \right], \quad u_{\text{ex}}(x) = \frac{2}{i \rho_0 \omega} P_0 \cos kx. \end{aligned} \quad (\text{B16})$$

4. Lower wall tangential oscillation both time-periodic and space-periodic

Lower wall oscillates tangentially with both time-periodic $e^{i\omega t}$ and space-periodic $\cos kx$, with a period T ($\omega = 2\pi/T$) and a wave-length $\lambda_g = 2\pi/k$. The wall velocity $u|_{y=0}$ is

$$U_w(t, x) = \Re \left[u_w \cos kx e^{i\omega t} \right] = u_w \cos kx \cos 2\pi(t/T), \quad k = 2\pi/\lambda_g, \quad (\text{B17})$$

where u_w is real, denoting the amplitude of wall oscillation. Figure 3 compares two velocity fields generated by two different stress fields for the same wall motion of (B17). The figure (a) on the left is the Stokes-type oscillatory layer (Eulerian + viscosity: under transparent gauge field):

$$u(t, x, y) = u_w \cos kx \Re \left[e^{i\omega t} \exp \left\{ -(i\omega/\nu)^{1/2} y \right\} \right], \quad (\text{B18})$$

derived from (41) ~ (43) of § V, with deleting $u_{\text{ex}}(x)$ and the sign reversed.

Next, the figure (b) on the right is the wavy layer obtained from the FGT system (FGT+viscosity under vectorial (colored) gauge field a_ν). One can see remarkable difference between the two fields.

ACKNOWLEDGMENTS

The author would like to express gratitude to the Royal Society and the journal *Philosophical Transactions of the Royal Society* for permission to use the FIG.1 and FIG.2 cited from [7] and FIG.5 cited from [6], both paper published ninety years ago.

The finite element analysis of the present study was carried out by the courtesy of Mr. Masanori Hashiguchi (Professional Engineer Japan; Former researcher of *i*CFD). Concerning the financial support to carry out the present study, the author would like to express heartfelt thanks to Mr. Kousuke Umadume, President of Institute of Japan Ship Model (WASEN).

REFERENCES RÉFÉRENCES REFERENCIAS

1. August Kundt, Ueber eine neue Art akustischer Staubfiguren und über die Anwendung derselben zur Bestimmung der Schallgeschwindigkeit in festen Körpern und Gasen, *Ann. der Physik & Chemie*, vol.127, 497 - 523 (1866).
2. Dvorak, *Ann. der Physik*, vol.153, 102 - 115 (1874);
3. V. Dvorak, *Ann. der Physik*, vol.157, 42 - 73 (1876).
4. J. W. S. Rayleigh, *The Theory of Sound*, Vol. Two (1896).
5. E. N. Da C. Andrade, Phenomena in a sounding tube, *Nature*, p.438, March 21 (1931).
6. E. N. Da C. Andrade, On the circulations caused by the vibration of air in a tube, *Proc. Roy. Soc. A*134, 445 - 470 (1931).
7. E. N. Da C. Andrade, On the groupings and general behaviour of solid particles under the influence of air vibrations in tubes, *Phil. Trans. Roy. Soc. A*230, 413-445 (1932).
8. R. A. Carman, Kundt Tube Dust Striations, *American J. of Phys.* 23, 505 - 507 (1955)
9. G. K. Batchelor, *The Theory of Homogeneous Turbulence*, Cambridge University Press (1953).
10. G. K. Batchelor, *An Introduction to Fluid Dynamics*, Cambridge University Press (1967).
11. James Lighthill, *Waves in fluids*, Cambridge University Press (1978).
12. L.D. Landau and E.M. Lifshitz, *Fluid Mechanics* (Pergamon Press, 2nd ed.) (1987).
13. T. Kambe, Fluid Gauge Theory. *Global Journal of Sci. Front. Res. A*, vol.21 (4), 113-147 (2021)
14. T. Kambe, Gauge symmetries in physical fields (Review), *Global Journal of Sci. Front. Res. A*, vol.21 (4), 1- 44.
15. R. Utiyama, Invariant theoretical interpretation of interaction, *Phys. Rev.* 101, 1597 - 1607(1956).
16. R. Utiyama, Introduction to General Gauge *Field Theory* [book in Japanese], (Iwanami, Tokyo) (1987).
17. Kambe T., New representation of rotational flow fields satisfying Euler's equation of an ideal compressible fluid, *Fluid Dyn. Res.* 45, 015505 (16pp) (2013).
18. Scofield D. F. and Pablo Huq, Fluid dynamical Lorentz force law and Poynting theorem – derivation and implications. *Fluid Dyn. Res.*, 46, 055514 (22pp) (2014).
19. Kambe T., New scenario of turbulence theory and wall-bounded turbulence: Theoretical significance, *Geophys. Astrophys. Fluid Dyn.* 111, 448-507, (2017).

20. Kambe T 2020 New perspectives on mass conservation law and waves in fluid mechanics, *Fluid Dyn. Res.* 52, 1 - 34 (2020).
21. Djouadi A. 2008: The anatomy of electro-weak symmetry breaking, I: The Higgs boson in the standard model, Phys. Rept. 457: 1-216; LPT-Orsay-05-18,
22. Laura Reina 2011: lectures on Higgs-Boson Physics, Proc. of TASI 2011, arXiv: 1208.5504 [hep-ph].
23. Y. Nambu, Spontaneous Symmetry Breaking in Particle Physics: A Case of Cross Fertilization, Nobel Lecture (2008).

Note Added in Proof:

The spontaneous symmetry breaking (SSB) is explained by the Nobel Laureate *Yoichiro NAMBU* in his Nobel Lecture [23] in 2008: ”*Spontaneous Symmetry Breaking in Particle Physics: A Case of Cross Fertilization*”, in which the following illustrative example is given:

”... In fact, it (*SSB*) is a very familiar one in our daily life. For example, consider an elastic straight rod (*of circular cross-section*) standing vertically. It has a rotational symmetry; it looks the same from any horizontal direction. But if one applies increasing pressure (*pressing stress*) to squeeze it, it will bend in some direction, and the symmetry is lost. The bending can occur in principle in any (*horizontal*) direction since all directions are equivalent. But you do not see it unless you repeat the experiment many times. This is *SSB*. ”

One can compare this example with our case of spontaneous symmetry transition in the Kundt’s experiment. The initial state of the elastic straight rod (of circular cross-section) standing vertically corresponds, in our case, to the acoustic pure resonance of wavelength λ_r in a closed tube, which is governed by the Euler’s equation of motion in a transparent gauge field $a_\nu^{(0)} = \partial_\nu \Psi$.

As the acoustic intensity increases, the gauge field a_ν shows spontaneously its appearance at a transition when the field a_ν is colored with a characteristic wave-length ℓ of transverse rotational waves, coexisting in the irrotational resonant acoustic waves of wave-length λ_r . The length ℓ is not unique, but depends on the fluid state concerning distribution and degree of the rotational component of the background fluid motion. This is analogous to the case of rod bending. The horizontal direction of bending depends on the internal microscopic structure within the elastic rod.

Thus, it is understood that the elastic rod could be an illustrative example to our Kundt’s experiment as well.